

A Computational Framework for Multiscale Modeling of the Mitral Valve

Chung-Hao Lee and Michael S. Sacks

Center for Cardiovascular Simulation
Institute of Computational Engineering and Sciences
Department of Biomedical Engineering
University of Texas at Austin, Austin TX 78712

Key Words: *Mitral valve, simulation.*

The mitral valve (MV) is one of the four heart valves which locates in between the left atrium and left ventricle and regulates the unidirectional blood flow and normal functioning of the heart during cardiac cycles. Alternation of any component of the MV apparatus will typically lead to abnormal MV function. Currently 40,000 patients in the United States receive MV repair or replacement annually according to the American Heart Association. Clinically, this can be achieved iteratively by surgical repair that reinstate normal annular geometry (size and shape) and restore mobile leaflet tissue, resulting in reduced annular and chordae force distribution. High-fidelity computer simulations provide a means to connect the cellular function with the organ-level MV tissue mechanical responses, and to help the design of optimal MV repair strategy. We present here the details of our first steps to create state-of-the-art of mitral valve modeling techniques, with an emphasis on what is known and investigated at various length scales. A modified left heart simulator was used for acquisition of the in-vitro mitral valve deformations at stress-free (referential), pressure loaded (~ 30 mmHg) and fully loaded (~ 70 mmHg) states (Fig. 1). The segmented MV geometry at each state was imported into Geomagic Studio (Morrisville, NC) for generation of the corresponding finite element model (Fig. 1-b, 6,528 four-node shell elements, in which 2,176 and 4,352 elements are for the MVAL and MVPL, respectively). The 3D locations of the key points for representation of the MV chordae tendineae, such as MV PM attaching points, chordal branching points, and MV leaflet attaching points, were quantified for realistic reconstruction of chordae tendineae (297 three-dimensional truss elements, Fig. 1-b). Moreover, spatially-varied and anatomically accurate MV leaflet thicknesses were determined from the Micro-CT data. Next, The collagen fiber micro-structural information, including the preferred fiber direction ϕ_f and OI value, was mapped onto the finite element model (Fig. 2-a and Fig. 2-b). Simulations of the MV systolic closure were performed in the FE commercial software ABAQUS 6.11 (SIMULIA, Providence, RI). The numerical predictions of the deformed geometry were in general agree well with the in-vitro experimental data, with the total displacement errors of 13.72 mm and 14.93 mm evaluated at the total 266 fiducial markers under pressures of 30 mmHg and 70 mmHg. The differences in marker displacements between the numerical results and experimental data were 0.388 ± 0.236 mm and 0.261 ± 0.192 mm at 30 mmHg, and 0.537 ± 0.336 mm and 0.411 ± 0.349 mm at 70 mmHg for the MVAL and MVPL, respectively. Moreover, the principal stretches in the radial and circumferential directions and in-plane Jacobian were captured well by the numerical simulations (Fig. 3). The predicted maximum values of λ_C , λ_R , and J_{2d} were 1.589, 1.216, 1.617 for the MVAL and 1.689, 1.208, 1.702 for the MVPL at 70 mmHg in comparison with the in-vitro measurements: $\lambda_C=1.601$, $\lambda_R=1.234$, and $J_{2d}=1.631$ for the MVAL and $\lambda_C=1.655$, $\lambda_R=1.224$, and $J_{2d}=1.695$ for the MVPL. We thus conclude that the improved accuracy of the current mapping techniques do indeed provide more accurate modeling results of the MV. This important result not only justifies these types of approaches, but more importantly will help us towards tissue-cell interactions, which drive the fundamental biologic response of the MV to repair.

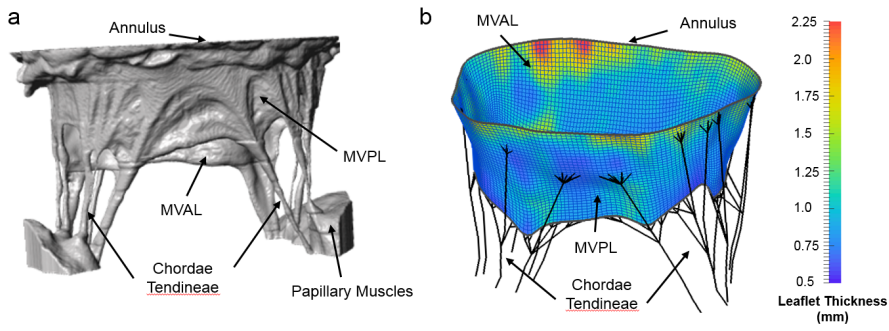


Fig. 1 (a) 3D reconstruction of anatomically accurate geometry of the mitral valve from high-resolution Micro-CT images, and (b) the corresponding finite element model (thin-shell elements for the MV leaflets and 3D truss elements for the MV chordae) with MV leaflet thicknesses determined based on the Micro-CT measurements.

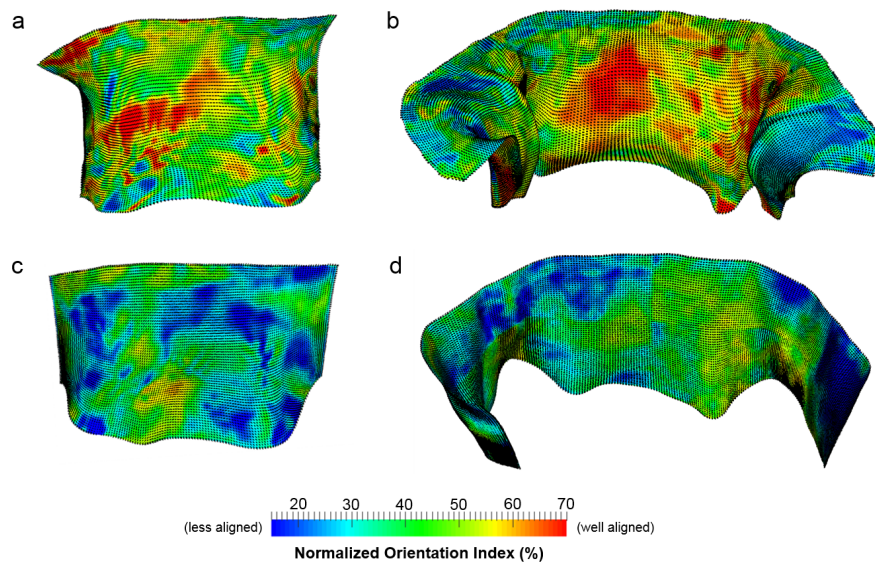


Fig. 2 Mapping of the collagen fiber micro-structural architecture onto the 3D finite element mesh at the deformed (fully-loaded) configuration Ω_t : (a) MVAL and (b) MVPL, and at the reference (stress-free) configuration Ω_0 : (c) MVAL and (d) MVPL.

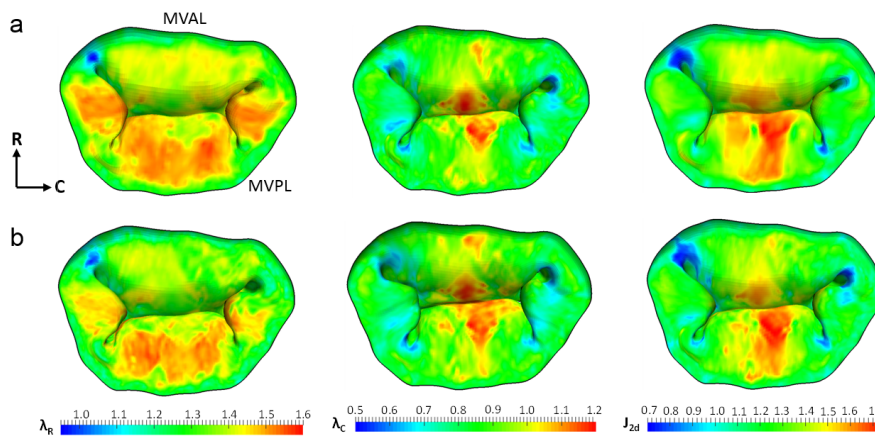


Fig. 3 Comparison of the principal stretches (λ_c and λ_R) and in-plane Jacobian (J_{2d}) at the fully-loaded state: (a) in-vitro measurements and (b) numerical results via FE simulations.

ACKNOWLEDGMENTS This research was supported by NIH grant R01 HL-089750.